TSINGHUA SCIENCE AND TECHNOLOGY
ISSN 1007-0214 05/20 pp684–697
DOI: 10.26599/TST.2023.9010054
Volume 29, Number 3, June 2024

Cost-Based Research on Energy Management Strategy of Electric Vehicles Using Hybird Energy Storage System

Juanying Zhou*, Jianyou Zhao, and Lufeng Wang

Abstract: This paper uses the minimization and weighted sum of battery capacity loss and energy consumption under driving cycles as objective functions to improve the economy of Electric Vehicles (EVs) with an hybrid energy storage system composed of power batteries and ultracapacitors. Furthermore, Dynamic Programming (DP) is employed to determine the objective function values under different weight coefficients, the comprehensive cost consisting of battery aging and power consumption costs, and the relationship between the hybrid power distribution. We also evaluate the real-time fuzzy Energy Management Strategy (EMS), fuzzy control strategies, and a strategy based on DP using the World Light vehicle Test Procedure (WLTP) driving cycle and a synthesis driving cycle derived from New European Driving Cycle (NEDC), WLTP, and Urban Dynamometer Driving Schedule (UDDS) as examples. Then, the proposed strategy is compared with the fuzzy control strategy and the strategy based on DP. Compared with fuzzy energy management strategy (namely FZY-EMS), the proposed EMS reduces the battery capacity loss and system energy consumption. The results demonstrate the effectiveness of the proposed EMS in improving EV economy.

Key words: automobile engineering; hybrid energy storage; Energy Management Strategy (EMS); fuzzy control strategy

1 Introduction

Relative to gasoline and diesel-powered vehicles, Electric Vehicles (EVs) have the advantages of energy saving, low noise, emission reduction, and simple power system structure, which give them a prominent place in sustainable transportation. EVs that use a Hybrid Energy Storage System (HESS)[1, 2] composed of an ultracapacitor and power batteries combine the advantages of these two forms of energy storage. Furthermore, HESS can protect the power battery, improve vehicle economy, and help overcome mileage anxiety[3, 4].

The power battery and ultracapacitor of HESSs act in tandem to store energy and provide power as needed. An Energy Management Strategy (EMS) can optimize system efficiency and improve vehicle economy. Typical EMSs include rule-based strategies[5–7] (e.g., logic rules and fuzzy logic[8–12]), intelligent algorithm based strategies (e.g., convex optimization[13] and genetic algorithm[14]), and global optimization algorithms (e.g., Dynamic Programming (DP)[15]). Particle Swarm Optimization (PSO) has attracted increasing research attention because of its simple mechanism, relatively small number of parameters, and the advantage of integrating with other algorithms to improve overall optimization performance[16].

Meanwhile, the power battery cost accounts for a

• Juanying Zhou is with School of Automobile, Chang'an University, Xi'an 710064, China, and also with College of Automotive Engineering and General Aviation, Shaanxi Vocational and Technical College, Xi'an 710038, China. E-mail: zhoujy@chd.edu.cn.
• Jianyou Zhao is with School of Automobile, Chang'an University, Xi'an 710064, China. E-mail: jyzhao@chd.edu.cn.
• Lufeng Wang is with College of Automobile, Shaanxi College of Communication Technology, Xi'an 710018, China. E-mail: lfwang@chd.edu.cn.
* To whom correspondence should be addressed.
Manuscript received: 2022-11-25; revised: 2023-03-24; accepted: 2023-05-31

substantial portion of the total cost of the whole vehicle. Furthermore, in the EMS design, the aging factor of the battery must also be fully considered to prolong its service life, and thereby improve the economy of the whole vehicle and the value of its entire life cycle[17]. In Ref. [2], DP was applied to match the parameters of the composite power supply and meet the optimization goals of minimizing the energy consumption of the composite power supply and the capacity loss of the battery pack. In Ref. [8], a rule-based control strategy was formulated, taking the total cost and total quality of the composite HESS as parts of the optimization goal, and a composite fuzzy control strategy was proposed. In Ref. [13], convex optimization was used to optimize the power distribution to achieve the optimization goal of determining the weighted sum of the initial cost and cost of the composite power supply. In Ref. [14], a multipart objective was established, to minimize both the replacement cost of the composite power supply and the average daily energy consumption. The optimization function uses a genetic algorithm to optimize the EMS of the composite power supply, based on which a rule-based EMS is presented. While the rule-based control strategy is simple, its optimization requires further improvement. Additionally, fuzzy control is robust and suitable for time-varying systems; however, its control strategy is mainly based on expert experience and is subjective. The use of optimization algorithms to optimize fuzzy controllers can more effectively adapt to changes in operating cycles[18–20]. HESSs are promising for renewable energy integration and EV adoption, as well as for the battery-supercapacitor hybrid system setup, Direct Current to Direct Current (DC-DC) converter design, and EMS development. A case study shows that an HESS with proper size and EMS may minimize battery deterioration by 40% at 1/8 the system cost. An EV operational data based battery capacity estimate system is proposed in the article. It outperforms state-of-the-art approaches with a mean absolute percentage error of 2.79% and minimal computational cost[21, 22]. The optimization problem's convexity must be considered when convex optimization is applied, which is difficult in practical application. Meanwhile, the genetic algorithm has a low convergence speed and can easily fall into a local minimum. Finally, although DP can achieve global optimization, it is slow.

Given the problems of poor optimization results, strong subjectivity, difficulty in actual use, and long calculation time of the above EMS, the current work takes an EV with batteries and ultracapacitors as the research object. The optimization goal is to minimize the weighted sum of battery capacity loss and energy consumption, and DP is used to solve the objective function under different weight coefficients. We also determine the comprehensive cost consisting of battery aging cost and energy consumption cost, and the corresponding power distribution relationship between the power battery and the ultracapacitor. Based on these results, we apply PSO to optimize fuzzy logic membership parameters, from which a real-time fuzzy EMS is developed.

2 Research Structure

The arrangement of this paper is shown in Fig. 1. Meanwhile, the remainder of the paper is presented as follows: Section 3 introduces the configuration characteristics of the model EV system with batteries and ultracapacitors. In Section 4, the World Light vehicle Test Procedure (WLTP) driving cycle is selected as the research driving cycle, and a synthesis of the New European Driving Cycle (NEDC), WLTP, and Urban Dynamometer Driving Schedule (UDDS) is selected as a verification driving cycle. In Section 5, we construct the objective function that minimizes the weighted sum of the capacity loss and energy consumption of the power battery under cycling, after which we use DP to solve the objective function value under different weight coefficients. In this section, we also introduce comprehensive cost as a measure of the EMS. It includes the purchase price of the battery pack and considers different electricity prices, which are assigned to the comprehensive cost with weight coefficients as the independent variable. Finally, we obtain the weight coefficient and the corresponding power distribution relationship when the comprehensive cost is the smallest. In Section 6, based on the above global optimization results, we use PSO to optimize fuzzy logic membership parameters, after which we develop a real-time fuzzy EMS. Section 7 discusses the fuzzy strategy and fuzzy control based on PSO in the WLTP and synthesis cycles. The proposed EMS, the fuzzy logic strategy, and the DP-based EMS are simulated and analyzed in this section. Then, we compare the proposed EMS with the fuzzy control strategy and the DP-based EMS. Finally, Section 8 presents the conclusions and points to future work.

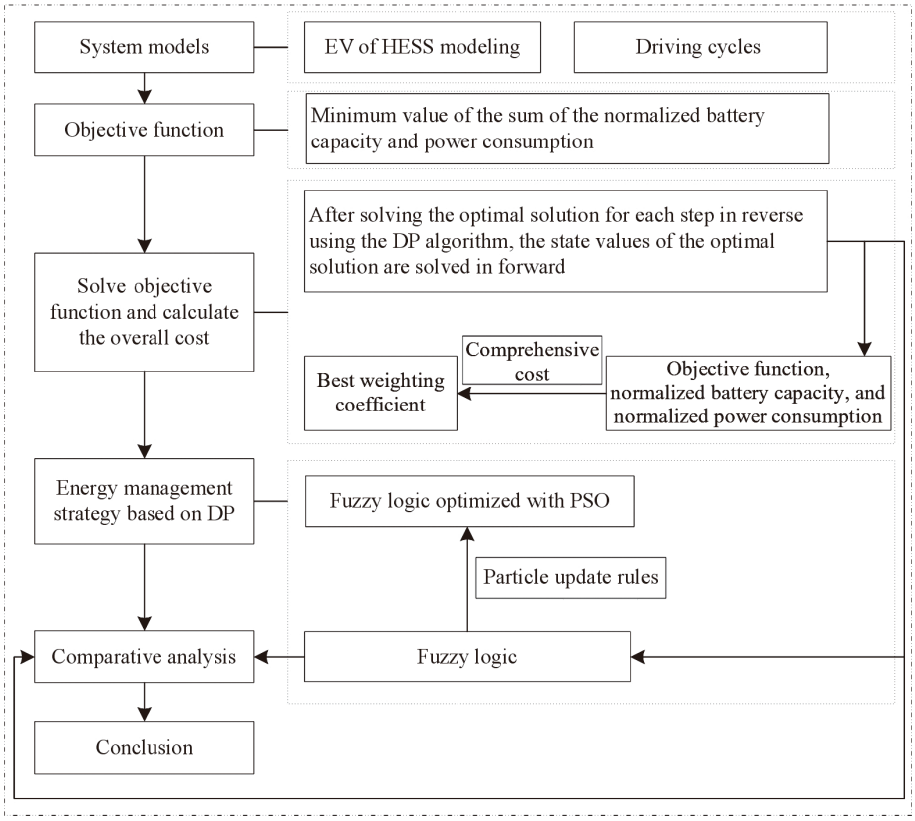

Fig. 1 Arrangement of this paper.

3 Composite Power EV Structure and Parameters

Ultracapacitors are energy storage devices that bridge the gap between batteries and conventional capacitors. They can store more energy than capacitors and supply higher power outputs than batteries. EVs that use HESSs typically use Electrochemical Double-Layer Capacitors (EDLCs) as the supercapacitor. Also known as supercapacitors or ultracapacitors, EDLCs are energy storage devices that can store and release large amounts of energy quickly. They have high power density and can provide short bursts of energy to help meet the demands of a vehicle's powertrain. Additionally, EDLCs have a longer cycle life and faster charging times than traditional batteries, making them well-suited for use in EVs.

3.1 Structure of hybrid energy storage system in an EV

There are many types of HESS. In our version of HESS, the ultracapacitor is connected in series with DC-DC, and connected in parallel with the battery pack to connect to the DC bus, thus providing the advantages of simple structure and convenient control. The structure is shown in Fig. 2. The EMS calculates the ultracapacitor output power and battery output power according to the collective State of Charge of the battery (SOC_b), the State of Charge of the ultracapacitor (SOC_u), and the power P[2].

3.2 Electric machine

We use a permanent magnet synchronous motor as the EM model. Its maximum speed is 8000 rpm, its maximum torque is 180 N·m, and its maximum power is 105 kW. The electric power of the drive motor can be expressed as a relationship between the motor output power and the motor efficiency,

$$P_{\text{em}} = \frac{T_m \cdot \omega_m}{9.55} \cdot \eta_m^z(T_m, \omega_m) \tag{1}$$

where P_{em} is the power of the EM, T_m is the torque, ω_m is the angular velocity, η_m is the EM's efficiency, which is expressed as a function of the torque and rotational speed, and z is the index coefficient; when $z = -1$, the machine works as a motor, and when $z = 1$, the machine works as a generator. In this paper, we perform the calculation in the form of a look-up table. The functional relationship is shown in Fig. 3.

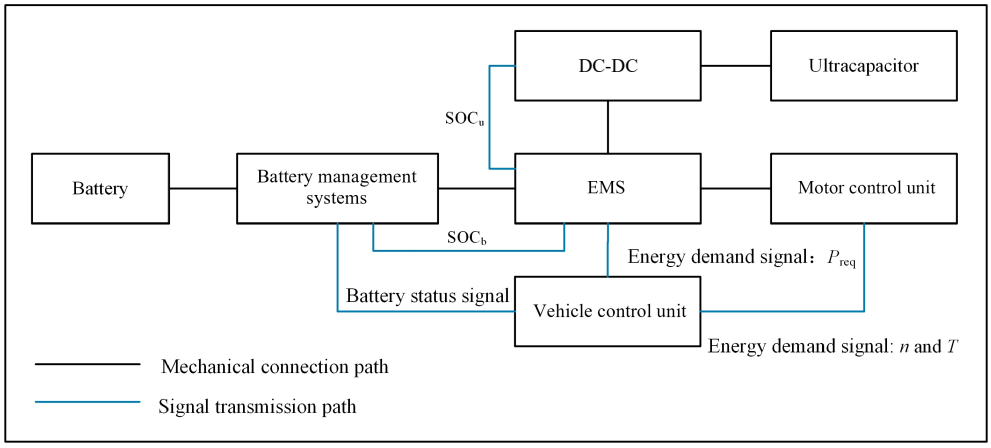

Fig. 2 Structure of hybrid energy storage system.

3.3 Power of the DC bus

The power of the DC bus is defined by

$$\begin{cases} P_{\text{dri}} = P_{\text{b}} + P_{\text{u}} \cdot \eta_{\text{DC-DC}}, \\ P_{\text{re}} = P_{\text{b}} + P_{\text{u}} / \eta_{\text{DC-DC}} \end{cases} \tag{2}$$

where P_{dri} is the driving power, P_{b} is the battery power, P_{u} is the ultracapacitor power, P_{re} is the bus power in the energy feedback, and $\eta_{\text{DC-DC}}$ is the DC-DC conversion efficiency, as shown in Fig. 4.

3.3.1 Ultracapacitor

The ultracapacitor model is shown in Fig. 5. The ultracapacitor has a nominal capacitance of 28 F and a rated voltage of 399 V. The ultracapacitor model is described by

$$U_{\text{u}} = U - I_{\text{u}} \cdot R_{\text{u}} \tag{3}$$

and the power of the ultracapacitor is given by

$$P_{\text{u}} = U_{\text{u}} \cdot I_{\text{u}} - I_{\text{u}}^2 \cdot R_{\text{u}} \tag{4}$$

where U_{u} is the output voltage of the ultracapacitor, U is the open-circuit voltage of the ultracapacitor, I_{u} is the current of the ultracapacitor (discharge is positive, charge is negative), and R_{u} is the capacitor equivalent internal resistance. The relationship between voltage and SOC is shown in Fig. 6.

3.4 Battery

3.4.1 Battery circuit model

The nominal capacity of the power battery pack is 102 A·h, and the total rated voltage is 400 V. The battery model adopts the Rint model of internal resistance voltage[17], as shown in Fig. 7. The Rint model is a mathematical model that simplifies the representation of a battery by assuming that it can be approximated as a voltage source in series with an internal resistor. The internal resistor represents the battery's internal resistance, while the voltage source represents its open-circuit voltage. This model is frequently used in battery management systems to monitor battery health and optimize performance, as well as in battery modeling and simulation to predict how batteries perform under different conditions. Notably, however, the Rint model is a simplified representation of the complex electrochemical

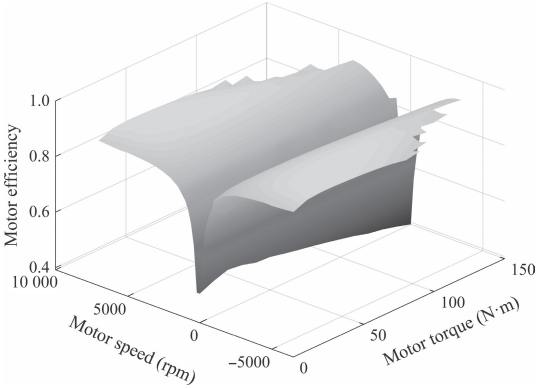

Fig. 3 Model of motor efficiency.

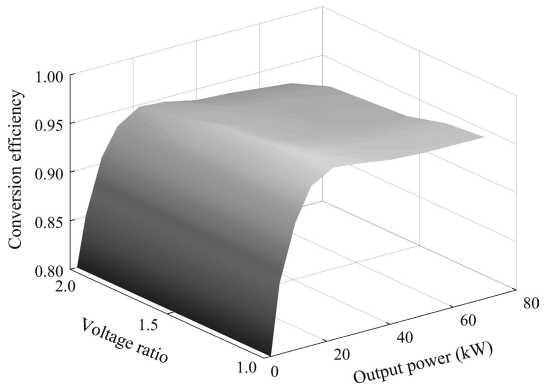

Fig. 4 Efficiency of DC-DC converter.

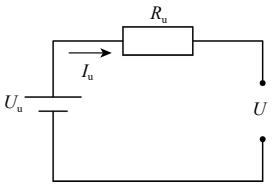

Fig. 5 Ultracapacitor model.

processes that occur within a battery, and its accuracy may be limited under certain conditions. The battery model can be described in the following:

$$U_b = U_0 - I_b \cdot R_b \tag{5}$$

The power of the battery is defined as

$$P_b = U_b \cdot I_b - I_b^2 \cdot R_b \tag{6}$$

where U_b is the battery voltage, U_0 is the open-circuit voltage of the battery, I_b is the battery current, and R_b is the internal resistance of the battery, which includes ohmic resistance, concentration polarization resistance, and charge transfer resistance. The relationship between battery internal resistance, SOC, and battery ambient temperature is shown in Fig. 8.

3.4.2 Battery thermal model

The Bernardi heat production model[23] is chosen to determine the temperature rise of the power battery. It can be defined as

$$\frac{dT}{dt} = \frac{R_b \cdot I_b^2}{m_b \cdot C_p} - \frac{T \cdot I_b}{m_b \cdot C_p}\frac{dE_0}{dT} \tag{7}$$

where dT/dt is the rate of change of the battery's kelvin temperature, m_b is the mass of the single battery, C_p is the equivalent kelvin specific heat capacity of the battery, T is the temperature of the battery, and dE_0/dT is the temperature rise coefficient of the battery. The thermal management system of the whole vehicle controls the ambient temperature of the battery. In this study, we refer to the thermal management system of the power battery of an EV model and set the maximum working temperature of the power battery to 35°C (308.15 K).

The HESS parameter values are shown in Table 1.

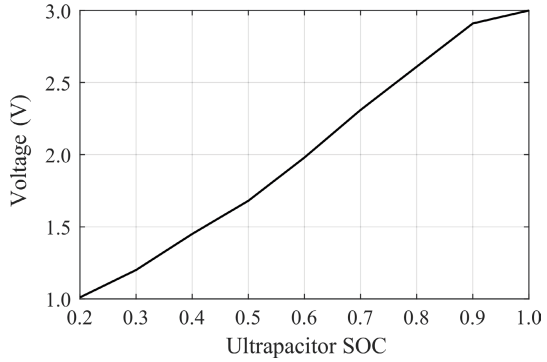

Fig. 6 Relationship between the voltage and SOC.

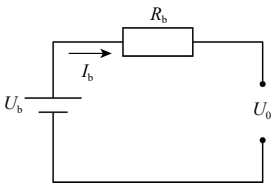

Fig. 7 Battery model.

3.5 Vehicle longitudinal dynamics

The required power of the vehicle is based on the formula governing the longitudinal force of the vehicle. We employ backward simulation to solve the driving power required by the vehicle through the speed and acceleration of each cycle. The required power P_{req} can be written as

$$P_{req} = \left(G \cdot f \cdot \cos\theta + A \cdot C_d \cdot \rho \cdot v^2/21.15 + \delta \cdot m \cdot \frac{dv}{dt} + G \cdot \sin\theta\right) v/(3600\,\eta_m^z) \tag{8}$$

where G is the weight of the vehicle, f is the rolling resistance, θ is the slope of the road, A is the windward area, C_d is the aerodynamic drag coefficient, ρ is the air density, v is the velocity of the vehicle, δ is the correction coefficient of the rotation mass, m is the gross mass of the vehicle ($G = mg$), and η_m is the efficiency of the drive train. The main parameters of the vehicle simulation model are provided in Table 2.

4 Driving Cycle Selection

The driving cycle, which describes the vehicle's speed

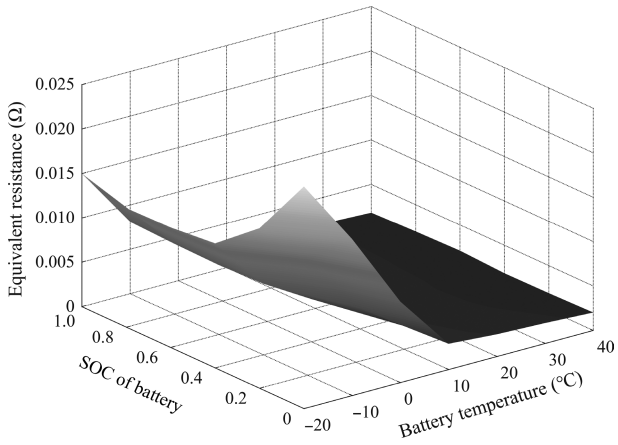

Fig. 8 Relationship among the battery SOC, equivalent resistance, and temperature.

over time, is the main benchmark for calibrating and optimizing various vehicle performance indicators. We use WLTP as the research driving cycle, where the maximum and average speed levels are 131.3 km/h and 46.5 km/h, respectively. The WLTP driving cycle is divided into low-, medium-, high-, and extremely high-speed according to the average driving speed, as shown in Fig. 9.

Next, we randomly select three different driving cycles (NEDC, UDDS, and WLTP), including urban, suburban, and expressways. We combine the representative speed range with a new driving cycle to verify the universality of the optimization effect of the proposed EMS. The synthesized driving cycles are composed of low-speed NEDC and WLTP driving cycles, medium-speed UDDS and WLTP driving cycles, and high-speed NEDC and UDDS driving cycles[24], as shown in Fig. 10.

5 Energy Management Strategy Based on Dynamic Programming (DP-EMS)

5.1 Objective function construction

The EMS of the vehicle composite power supply, which seeks to balance battery life and energy consumption, is one of the key factors in improving vehicle performance. By introducing the weight coefficient α, we construct an objective function to minimize the weighted sum of the battery's capacity loss and energy consumption under driving cycles,

$$\min J = f(\alpha, L(k)) = \alpha \cdot Q_{\text{loss}}^{\text{nor}} + (1-\alpha)\, E^{\text{nor}} \tag{9}$$

where J is the objective function, α is the weight coefficient (whose value ranges from 0 to 1), L is the sequence of control variables, $Q_{\text{loss}}^{\text{nor}}$ is the capacity loss of the battery, and E^{nor} is the normalized cyclic energy consumption of HESS. In addition, $Q_{\text{loss}}^{\text{nor}}$ and E^{nor} can be described as

$$\begin{cases} Q_{\text{loss}}^{\text{nor}} = \dfrac{Q_{\text{loss}} - Q_{\text{loss}}^{\min}}{Q_{\text{loss}}^{\max} - Q_{\text{loss}}^{\min}}, \\ E^{\text{nor}} = \dfrac{E - E^{\min}}{E^{\max} - E^{\min}} \end{cases} \tag{10}$$

where

$$\begin{cases} Q_{\text{loss}} = B \cdot \exp\left(\dfrac{-31700 + 163.3 \cdot I_{\text{b}}}{R \cdot T}\right) \cdot \text{AH}^{0.57}, \\ E = \int_{t_0}^{t_f} P_{\text{b}}(\tau)\, \text{d}\tau + \int_{t_0}^{t_f} P_{\text{u}}(\tau)\, \text{d}\tau \end{cases} \tag{11}$$

in which the superscripts "min" and "max" represent the minimum and maximum values of the variables they refer to, respectively; B is a pre-exponential factor, R is the gas constant, 8.314; T is the battery temperature expressed in Kelvins; t_0 and t_f are the trip start and end time, respectively; and AH is the Ah-throughput, described below:

$$\text{AH} = \int_{t_0}^{t_f} \sigma\,(I(\tau), T(\tau), \text{SOC}_{\text{b}}(\tau)) \cdot I(\tau)\, \text{d}\tau \tag{12}$$

where $\sigma(\,)$ is the severity factor which can be obtained empirically below:

Table 1 Hybrid energy storage system parameter value.

Parameter	Value
Series number of batteries	108
Parallel number of batteries	34
Series number of ultracapacitors	133
Parallel number of ultracapacitors	1

Table 2 Main parameters of the vehicle simulation model.

Parameter	Value
Mass of the vehicle m (kg)	1400
Friction and vertical force ratio f (%)	1
Windward area A (m^2)	1.60
Aerodynamic drag coefficient C_d	0.30
Air density ρ (kg/m^3)	1.18
Correction coefficient of the rotation mass δ	1.10
Efficiency of the drive train η_m	0.95

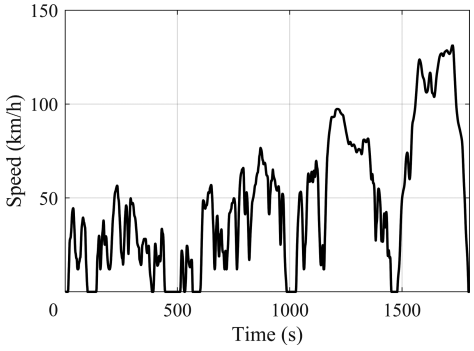

Fig. 9 WLTP driving cycle.

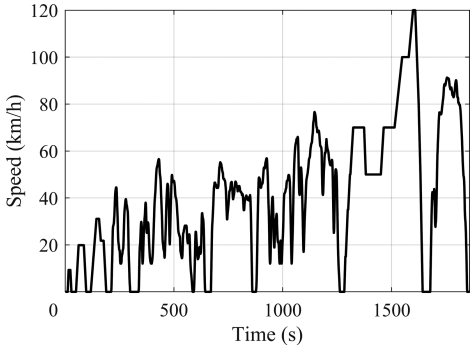

Fig. 10 Synthesis driving cycle.

$$\sigma(I,\ T,\ \mathrm{SOC_b}) = \left[\frac{(\beta\cdot\mathrm{SOC_b}+\gamma)\cdot\exp\left(\dfrac{-31700+163.3\cdot I_\mathrm{b}}{R\cdot T}\right)}{(\beta\cdot\mathrm{SOC_{nom}}+\gamma)\cdot\exp\left(\dfrac{-31700+163.3\cdot I_\mathrm{nom}}{R\cdot T_\mathrm{nom}}\right)}\right]^{\frac{1}{0.57}} \tag{13}$$

where β and γ are the fitting coefficients related to $\mathrm{SOC_b}$ ($\beta = 1385.5$ and $\gamma = 4193.2$). Additionally, $\mathrm{SOC_{nom}}$, T_nom, and I_nom are the SOC, temperature, and current of the battery in nominal cycles, respectively. In this study, $\mathrm{SOC_{nom}} = 0.35$, $T_\mathrm{nom} = 298.15$ K, and $I_\mathrm{nom} = 0.35$ A.

5.2 Dynamic programming

The core concept of DP is to ensure that the optimization problem achieves the globally optimal solution by transforming a complex multistage globally optimal decision problem into a multistage local optimal problem, and by obtaining the optimal solution of each stage separately. According to the optimal control theory of DP[25, 26], the discrete form of the DP iterative format with the optimization objective function as the performance index is

$$J_k(L(h)) = \begin{cases} \min\left(\alpha\cdot Q_\mathrm{loss}^\mathrm{nor}+(1-\alpha)\cdot E^\mathrm{nor}\right), & k = k_\mathrm{end};\\ \min\left(\alpha\cdot Q_\mathrm{loss}^\mathrm{nor}+(1-\alpha)\cdot E^\mathrm{nor}+J_{k+1}(L(h))\right), & k = k_\mathrm{end}-1, k_\mathrm{end}-2,\ldots,1 \end{cases} \tag{14}$$

where $J_k(L(h))$ is the objective function with the variable h in the stage k, and k_end denotes the final stage. In this work, $L \in [0:0.01:1]$, α is substituted into Eq. (9) to solve the objective function value under different weight coefficients, as shown in Fig. 11. Thus, we are able to obtain the capacity loss of the battery and the system cycle energy consumption, as shown in Fig. 12. The WLTP driving cycle and the synthesis driving cycle are the two types of driving cycles used to obtain the optimal solution variable and values of the battery loss and energy consumption in different weight co-efficients (i.e., 0–1). The graphical representations of the obtained results are indicated in Figs. 11 and 12. The WLTP is a standardized driving cycle designed to assess the fuel consumption, CO_2 emissions, and pollutant emissions of light-duty vehicles. It replaces the outdated NEDC in 2017. The WLTP consists of four driving phases with different speed, acceleration, and deceleration patterns, covering a distance of 23.25 km (14.44 miles) within 30 min. It

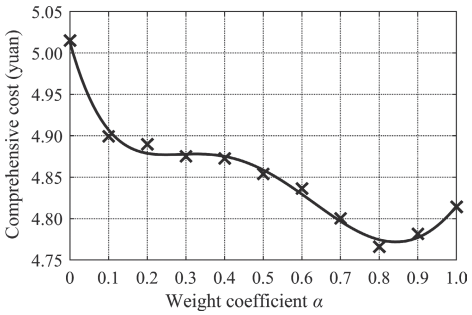

Fig. 11 Optimal solution variable with different weight coefficients.

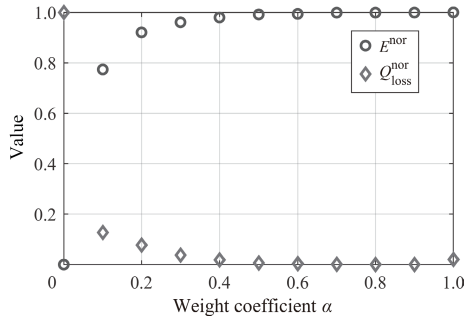

Fig. 12 Value of battery loss and energy consumption with different weight coefficients.

represents a controlled environment that allows for a consistent and accurate comparison among different vehicles.

At the same time, the synthesis driving cycle is a generic driving cycle that represents real-world driving conditions in a particular region or country. It is a statistical analysis of driving data that provides an average of typical driving scenarios. The synthesis driving cycle is used for vehicle emissions and fuel consumption evaluation in several regions, including the United States, Japan, and China. Unlike the WLTP, the synthesis driving cycle is not standardized and varies depending on the duration, region, and distance covered. It generally covers a longer distance and duration, including more stops and starts to better reflect real-world driving conditions.

On the one hand, when $\alpha = 0$, the optimization goal is based completely on the system cycle energy consumption. At this point, the system cycle energy consumption is the least, the battery capacity loss is the greatest, and the composite power system is closest to the working state of a single battery. On the other hand, when $\alpha = 1$, the optimization goal is based completely on the battery life. The battery capacity loss becomes the smallest, and the system cycle energy consumption becomes the largest.

5.3 Solute optimal weight coefficient based on comprehensive cost

The comprehensive cost is the sum of battery aging cost and power consumption cost. The former is the purchase cost of the battery pack shared by the loss of the battery capacity in the current trip, while the latter is the power consumption cost of the power battery and the output power of the ultracapacitor. This can be described as

$$F_c = C_{br} + C_e \tag{15}$$

where F_c is the comprehensive cost, C_{br} is the battery aging cost, and C_e is the energy consumption cost, C_{br} and C_e are defined in Eq. (16), shown at the bottom of this page.

In Eq. (16), P_{br} is the battery pack acquisition cost (1000 yuan/(kW·h)), $Q_{EOL\%}$ is the capacity loss percentage when the battery is at end of its life, and p_e is the electricity price. The cost of electricity consumption is related to the unit price of electricity. Taking Xi'an as an example, the price of commercial AC-slow charging is 0.8 yuan/(kW·h), and the DC-fast charging price ranges from 1.0 to 1.5 yuan/(kW·h). Substituting the battery capacity loss and system cycle energy consumption under different weight coefficients into Eqs. (16) and (17), the fitting formula is found in Eq. (17), shown at the bottom of this page, where F_{c1} is the comprehensive cost of AC-slow charging with an electricity price of 0.8 yuan/(kW·h); and F_{c2} and F_{c3} are the comprehensive costs with electricity prices of 1.0 and 1.5 yuan/(kW·h), respectively, for AC-slow charging and DC-fast charging.

The combined costs of different electricity prices are shown in Fig. 13. Taking the AC-slow charging price ($p_{e1} = 0.8$) as an example, when $\alpha = 0.78$, the minimum comprehensive cost per cycle is 3.34 yuan; when the DC-fast charging price $p_{e2} = 1.0$ is taken as an example, and with $\alpha = 0.81$, the minimum comprehensive cost per cycle is 3.68 yuan. When the fast charging price $p_{e2} = 1.5$, with $\alpha = 0.83$, is adopted, the minimum comprehensive cost per cycle is 4.53 yuan. The research object of this paper is commercial vehicles that require high charging speeds. Therefore, we consider the lowest comprehensive cost when the DC-fast charging price is $p_{e1} = 1.5$ and $\alpha = 0.83$.

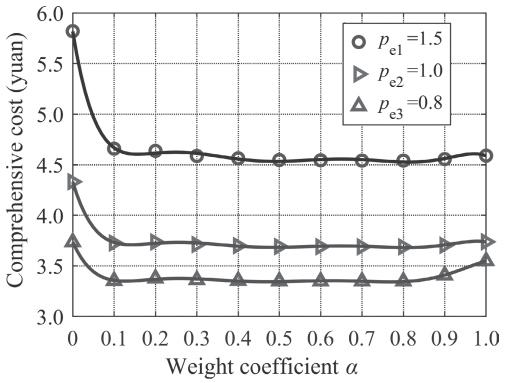

Fig. 13 Comprehensive cost for different electric prices and weight coefficients.

6 Energy Management Strategy Optimization

The optimal EMS obtained by DP cannot be applied in real-time, but its optimization result can be used to evaluate the effect of the EMS.

6.1 Fuzzy rules

Fuzzy control is suitable for multi-objective, nonlinear, time-varying systems, and has wide applicability. In this paper, we adopt the Mamdani-type fuzzy controller and use "If..., then..." statements to establish fuzzy rules. Here, each strategy is established individually because the driving and feedback states have different

$$\begin{cases} C_{br} = \dfrac{p_{br}\displaystyle\int_{t_0}^{t_f}(\beta\cdot \mathrm{SOC_b}(\tau)+\gamma)\cdot\exp\left(\dfrac{-31700+163.3\cdot I_b(\tau)}{R\cdot T(\tau)}\right)\cdot \mathrm{AH}(\tau)^{0.57}\,\mathrm{d}\tau}{Q_{EOL\%}}, \\ C_e = \dfrac{p_e\displaystyle\int_{t_0}^{t_f}(P_b(\tau)+P_u(\tau))\,\mathrm{d}\tau}{3.6\times 10^6} \end{cases} \tag{16}$$

$$\begin{bmatrix} F_{c1} \\ F_{c2} \\ F_{c3} \end{bmatrix} = \begin{bmatrix} -171.2 & 655.2 & -1008.3 & 800.1 & -348.1 & 81.1 & -9.1 & 3.7 \\ -215.9 & 835.9 & -1308.9 & 1062.4 & -475.4 & 115.0 & -13.7 & 4.3 \\ -369.2 & 1434.8 & -2259.0 & 1847.9 & -836.5 & 206.2 & -25.4 & 5.8 \end{bmatrix} \begin{bmatrix} \alpha^7 \\ \alpha^6 \\ \vdots \\ \alpha^2 \\ 1 \end{bmatrix} \tag{17}$$

logic. The input variables of the fuzzy policy-driven state are SOC_u and P_{dri}, whereas the input variables of the feedback state are SOC_b, SOC_u, and P_{re}. The domain of discourse of SOC_b is from 0.2 to 1, the domain of discourse of SOC_u is from 0.4 to 1, and the fuzzy subsets are divided into L, M, and H, representing low, medium, and high, respectively. In addition, the domains of the discourse of P_{dri} and P_{re} both range from 0 to 1, and the fuzzy subsets are divided into SL, L, M, H, and SH, representing represent extremely low, low, medium, high, and extremely high, respectively. The membership functions of SOC_b, SOC_u, and P_{dri} are shown in Fig. 14. The load ratio in Fig. 14c represents the normalized required power.

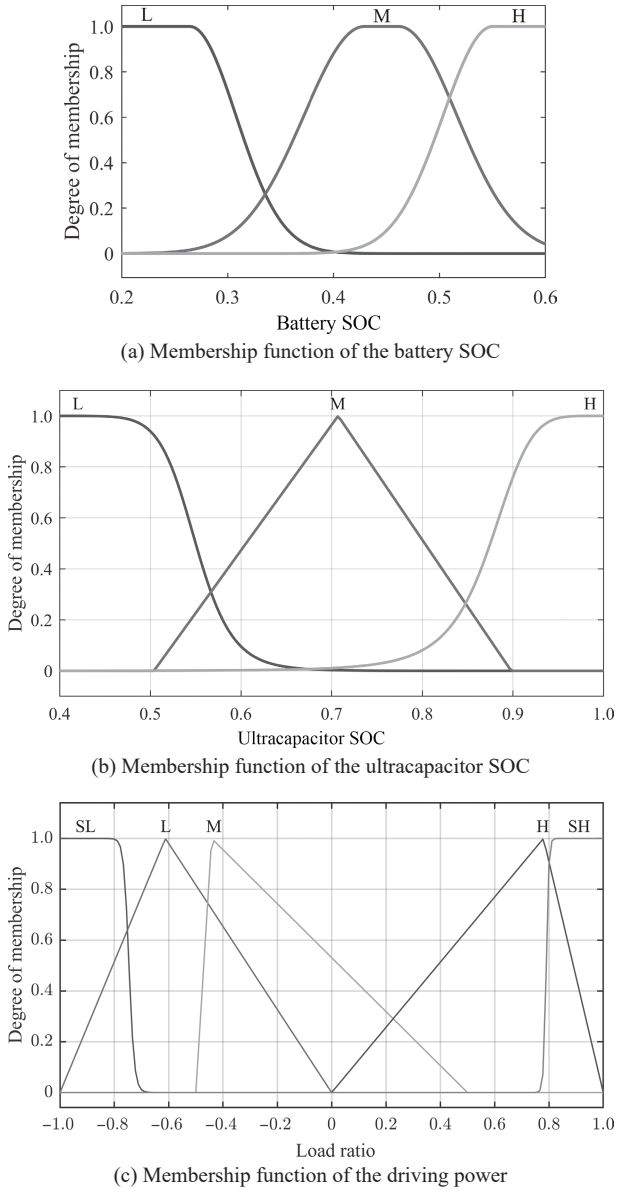

(a) Membership function of the battery SOC

(b) Membership function of the ultracapacitor SOC

(c) Membership function of the driving power

Fig. 14 Membership functions of driving status inputs.

The output gain coefficient is the proportionality coefficient of the ultracapacitor in the required power; its universe of discourse ranges from 0 to 1; and the fuzzy subset is divided into SL, L, M, H, and SH. The membership function rule is that the ultracapacitor and the battery work together when the battery is sufficiently charged, thereby reducing the charge and discharge current of the battery when the power demand is high, and the fuzzy control strategy avoids the charging and discharging of the ultracapacitor and DC-DC when the power demand is low. The energy feedback to the battery is given priority when the SOC_b is slow. The rules are shown in Tables 3 and 4. We refer to the fuzzy control strategy as "FZY-EMS" in this work.

6.2 PSO algorithm to optimize fuzzy strategy

The membership function of the above fuzzy control strategy depends on the subjective experience of experts; thus, the rules may not be optimal. Thus, we use PSO in this paper to optimize the fuzzy control. We iterate the objective function when the weight coefficient is 0.47, and then apply the optimized membership function to the energy distribution of the composite power system. The fuzzy strategy subjected to PSO is called "PFZY-EMS" in this work.

Theoretically, the more parameters that the PSO algorithm optimizes, the more chances it has to achieve what is known as the globally optimal solution. However, the particle swarm rules and the number of

Table 3 Driving state fuzzy control rules.

P_{dri}	$SOC_b \in L$			$SOC_b \in M$			$SOC_b \in H$		
	L	M	H	L	M	H	L	M	H
SL	SL	SL	SL	SL	SL	SL	SL	SL	SL
L	SL	SL	SL	SL	SL	SL	L	L	L
M	SL	M	H	SL	L	H	L	M	H
H	L	M	H	SL	M	H	L	H	H
SH	L	H	SH	L	H	SH	SL	H	SH

Table 4 Energy recovery fuzzy control rules.

P_{re}	$SOC_b \in L$			$SOC_b \in M$			$SOC_b \in H$		
	L	M	H	L	M	H	L	M	H
SL	SL	SL	SL	ML	SL	SL	M	SL	SL
L	SL	SL	SL	SH	M	SL	SL	SH	SH
M	SL	SL	SL	SH	M	L	SH	H	M
H	SL	SL	SL	SH	M	L	SH	SH	M
SH	SL	SL	SL	SH	M	SL	SH	SH	M

iterations also increase as the number of parameters increases, eventually leading to a substantial increase in computation time. Thus, we maintain the original fuzzy rules, and the membership function of the rule boundary is removed by PSO optimization.

First, we uniformly encode the parameters to be optimized. When the boundary of P_{dri} is removed, the membership parameters to be optimized are recorded as P_{dri1}, P_{dri2}, …, P_{dri11}. When the SOC_{u} boundary is removed, the membership parameters to be optimized are recorded as SOC_{u1}, SOC_{u2}, SOC_{u3}, and SOC_{u4}. At the same time, when the SOC_{b} boundary is removed, the membership parameters to be optimized are recorded as SOC_{b1}, SOC_{b2}, SOC_{b3}, and SOC_{b4}, while the membership parameters to be optimized for P_{re} are recorded as P_{re1}, P_{re2}, …, P_{re11}. So, 38 parameters need to be optimized. The steps to optimize fuzzy rule parameters using PSO are as follows:

Step 1: Take optimization variables $X = (P_{\text{dri1}}, P_{\text{dri2}}, \ldots, P_{\text{dri11}}, \text{SOC}_{\text{u1}}, \text{SOC}_{\text{u2}}, \ldots, \text{SOC}_{\text{u4}}, \text{SOC}_{\text{b1}}, \text{SOC}_{\text{b2}}, \ldots, \text{SOC}_{\text{b4}}, P_{\text{re1}}, P_{\text{re2}}, \ldots, P_{\text{re11}})$ as particles. Each dimension is encoded with real numbers, and the velocity and position of each particle are randomly initialized within their respective ranges.

Step 2: Decode each particle, output it to the fuzzy control rule as the corresponding membership parameter, and simulate the constructed pure EV model.

Step 3: Update the particle velocity and position by evaluating the current optimal position and the optimal position of the entire particle swarm using the following equations:

$$\begin{cases} v_i^{t'} = w \cdot v_i^{t'-1} + c_1 \cdot \text{rand} \cdot \left(p_{\text{best}} \cdot t_i^{t'-1} - x_i^{t'-1}\right) + \\ \qquad c_2 \cdot \text{rand} \cdot \left(g_{\text{best}} \cdot t_i^{t'-1} - x_i^{t'-1}\right), \\ x_i^{t'} = x_i^{t'-1} + v_i^{t'-1} \end{cases} \tag{18}$$

where w is the inertia factor, v_i is the particle speed, x_i is the current position of the particle, rand is a random number between 0 and 1, c_1 and c_2 are learning factors (with $c_1 = c_2 = 2$ in this study), and i and t' are the particle number, and the number of iterations, respectively. p_{best} and g_{best} are the self-optimal position and group-optimal position, respectively.

Step 4: Return to Step 3 to continue the iteration until the number of iterations does not change for 400 consecutive generations, and then use g_{best} as the optimal parameter of the fuzzy control rule. The drive state input membership function optimized by PSO is shown in Fig. 15. The load ratio in Fig. 15c represents the normalized required power.

Simulation results of the three energy management strategies under the two driving cycles are shown in Fig. 16. For each part, the results for the WLTP cycle are on the left, and those for the synthesis cycle are on the right.

7 Result and Analysis

Taking WLTP and synthesis driving cycles as examples, we analyze the PSO-based fuzzy EMS and

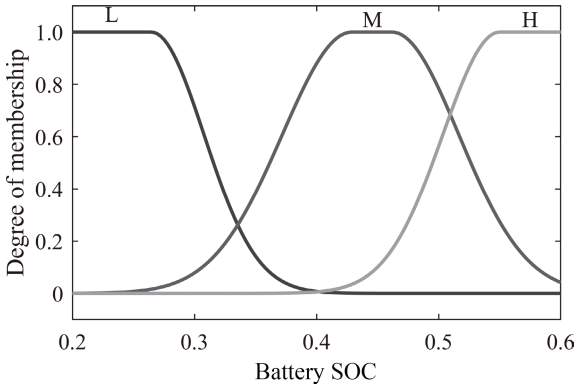

(a) Membership function of the battery SOC

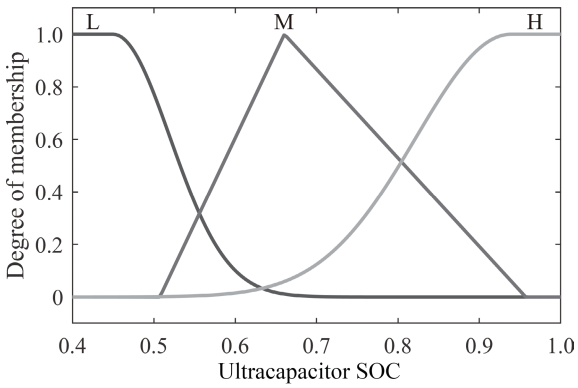

(b) Membership function of the ultracapacitor SOC

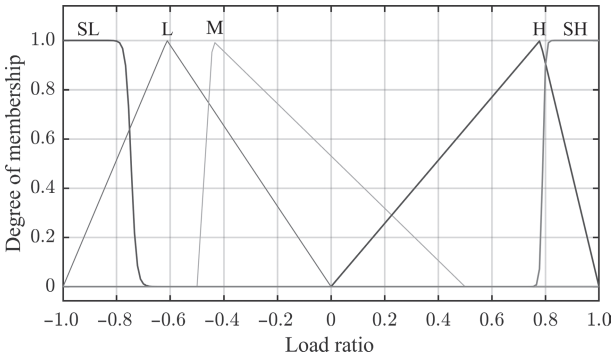

(c) Membership function of the driving power

Fig. 15 Membership functions of driving state inputs after particle swarm optimization optimization.

compare this with the fuzzy control and energy management strategies based on DP. The simulation results are shown in Figs. 16 and 17.

The output power of the battery for three energy management strategies and two driving cycles is shown in Fig. 16. It can be seen that the EMS of the PSO fuzzy control proposed in this paper effectively avoids a high current charge and discharge of the battery pack, which slows the aging process of the battery pack, and is closer to the energy management curve based on DP. Meanwhile, Fig. 17 compares the simulation results of three energy management strategies, namely, PFZY-EMS, FZY-EMS, and DP-EMS, for two driving cycles.

Figure 17a shows the battery capacity loss as a function of time. For the WLTP cycle, the battery capacity loss for PFZY-EMS lies initially (0–680 s) between the losses for DP-EMS and FZY-EMS, closer to DP-EMS and much lower than that of FZY-EMS. From 681 s to the end of the cycle, the battery capacity loss for the PFZY-EMS cycle is the least. For the synthesis cycle, the battery capacity loss of PFZY-EMS is much lower than that of FZY-EMS, and slightly higher than that of DP-EMS. At the end of the cycle, under the WLTP cycle, the battery capacity losses of the three strategies are $0.878\times10^{-3}\%$, $1.161\times10^{-3}\%$, and $0.9\times10^{-3}\%$ for PFZY-EMS, FZY-EMS, and DP-EMS, respectively. For the synthesis cycle, the corresponding battery capacity losses of these three strategies are $0.849\times10^{-3}\%$, $1.091\times10^{-3}\%$, and $0.832\times10^{-3}\%$, respectively. For this cycle, the PFZY-based strategy outperforms the FZY-based strategy, and is slightly inferior to the DP strategy. The energy consumption trends of the three systems for the two driving cycles are shown in Fig. 17b. The graphs indicate that for the WLTP cycle, the system energy consumption of PFZY-EMS is between those of DP-EMS and FZY-EMS from the start of the vehicle operation to 928 s. Meanwhile, from 929 s to the end of the cycle, the system energy consumption for PFZY-EMS is higher than those for the other two strategies. For the synthesis cycle, the system energy consumption of PFZY-EMS is between those of DP-EMS and FZY-EMS from 0 to 1068 s; its system energy consumption is the greatest from 1069 s to the end of the cycle. At the end of the cycle, under the WLTP cycle, the energy consumption levels of PFZY-EMS, FZY-EMS, and DP-EMS are 6.273×10^6 J, 5.98×10^6 J, and 5.962×10^6 J, respectively, while under the synthesis cycle, the corresponding cycle energy consumptions are 5.584×10^6 J, 5.327×10^6 J, and 5.036×10^6 J. The comprehensive cost trends of PFZY-EMS, FZY-EMS, and DP-EMS for two driving cycles are shown in Fig. 17c. At the end of the WLTP cycle, the comprehensive costs of PFZY-EMS, FZY-EMS, and DP-EMS are 4.569 yuan, 5.074 yuan, and 4.490 yuan, respectively. At the end of the synthesis cycle, the

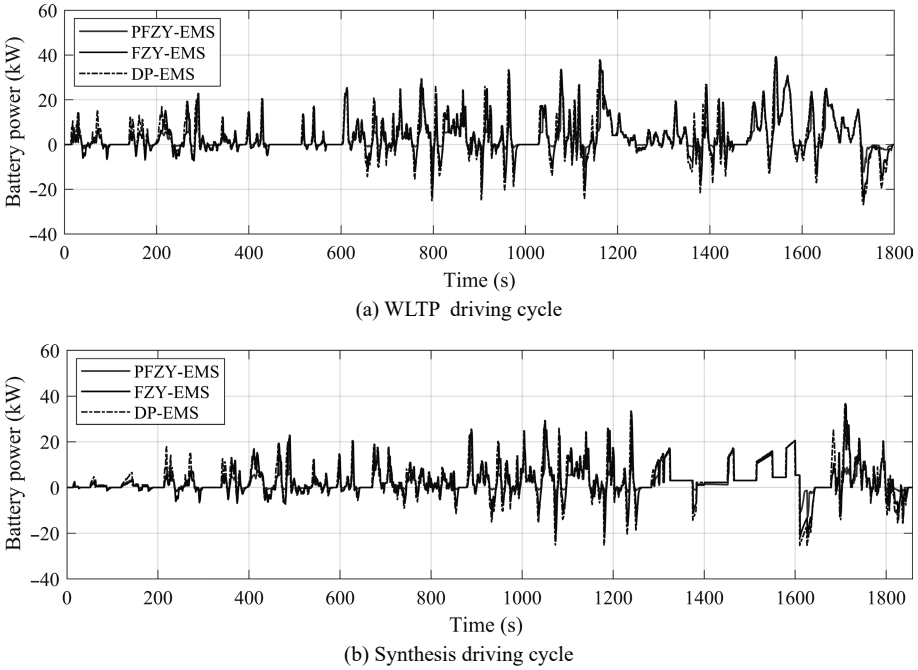

(a) WLTP driving cycle

(b) Synthesis driving cycle

Fig. 16 Membership functions of driving status inputs.

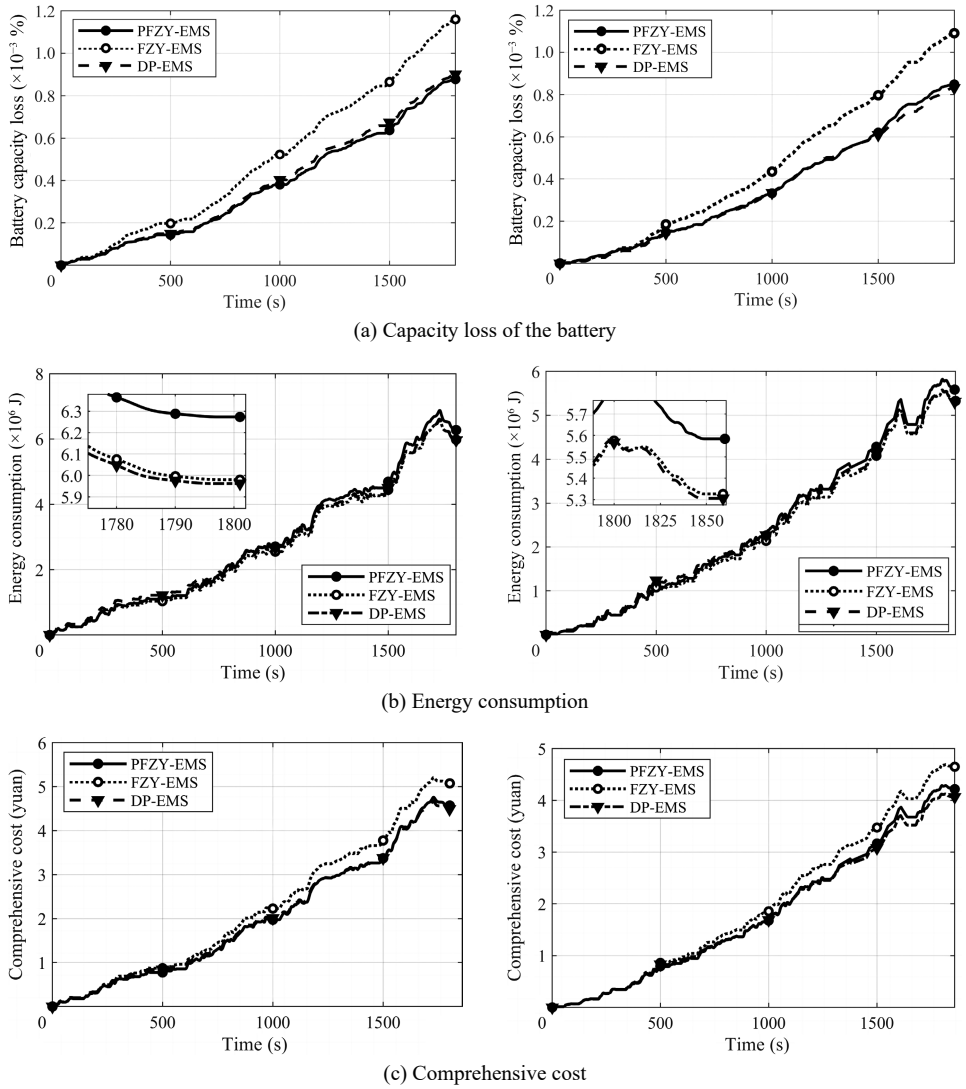

Fig. 17 Simulation results of three EMSs under two driving cycles. For each part, results for the WTLP cycle are on the left and for the synthesis cycle on the right.

corresponding cycle energy consumption levels of the three strategies are 4.217 yuan, 4.649 yuan, and 4.063 yuan, respectively. The cycle energy consumption of PFZY strategy is higher than those of the other two strategies. The reason is that the optimization objective function in this work is the comprehensive cost, and the battery aging cost is much higher than the energy consumption cost. Thus, the proposed EMS greatly reduces the capacity loss of the power battery and the comprehensive cost of the composite power supply at a small energy consumption cost.

Furthermore, the numerical results are shown in Table 5. Compared with FZY-EMS and DP-EMS, the EMS proposed in this paper reduces the battery capacity loss by 24.374% and 22.181%, and the system energy consumption increases by 4.900% and 4.824%, respectively. Comprehensive costs decreased by

Table 5 Comparison of evaluation indicators.

Strategy	Battery capacity loss (%)		Energy consumption ($\times 10^6$ J)		Comprehensive cost (yuan)	
	WLTP	Synthesis	WLTP	Synthesis	WLTP	Synthesis
PFZY-EMS	0.878×10^{-3}	0.849×10^{-3}	6.273	5.584	4.569	4.217
FZY-EMS	1.161×10^{-3}	1.091×10^{-3}	5.980	5.327	5.074	4.649
DP-EMS	0.900×10^{-3}	0.832×10^{-3}	5.962	5.036	4.490	4.063

9.953% and 9.292%, respectively. Meanwhile, compared with DP-EMS, the battery capacity loss is reduced by 24.374% under the WLTP cycle, and the battery capacity loss is increased by 2.043% under the synthesis cycle, and the system energy consumption is increased by 5.216% and 10.882%, respectively. The comprehensive cost also increased by 1.759% and 3.790%, respectively. Thus, the results of the PSO-optimized fuzzy EMS are much higher than those of the fuzzy control strategy, and slightly lower than those of the DP strategy, thus showing significant benefits.

8 Conclusion

The EMSs proposed in existing works are known for poor optimization results, strong subjectivity, difficulty in actual use, and long calculation time requirements. Thus, the present work uses an EV with batteries and ultracapacitors. In particular, this work investigates the energy management of EVs with an HESS. The weighted sum of the battery capacity loss and energy consumption under sample driving cycles is taken to minimize the objective function, which is then solved by DP. Thereafter, we obtain the objective function value under the weight coefficient, along with the corresponding composite power distribution relationship and the comprehensive cost composed of battery aging cost and power consumption cost. We then use the PSO algorithm to optimize the fuzzy logic membership parameters, after which we develop a real-time fuzzy EMS based on these optimization results. PFZY-EMS, FZY-EMS, and DP-EMS are then compared and analyzed in the research and verification cycles. The results demonstrate the effectiveness of the proposed EMS. However, the proposed EMS has not been verified in actual vehicles. In follow-up work, a test system will be built to conduct performance tests, and the strategy will be continuously optimized according to the test results.

Acknowledgment

This work was supported by the National Key Research and Development Program of China (No. 2020YFB1600400) and the Scientific Research Project of the Department of Transport of Shaanxi Province (No. 18-27R).

References

[1] B. Zhao, Q. Song, and W. Liu, Power characterization of isolated bidirectional dual-active-bridge DC-DC converter with dual-phase-shift control, *IEEE Trans. Power Electron*, vol. 27, no. 9, pp. 4172–4176, 2012.

[2] C. X. Song, F. Zhou, and F. Xiao, Energy management optimization of Hybrid Energy Storage System (HESS) based on dynamic programming, (in Chinese), *J. Jilin Univ.* (*Eng. Technol. Ed.*), vol. 47, no. 1, pp. 8–14, 2017.

[3] D. Z. Yao, C. J. Xie, T. Zeng, and L. Huang, Multi-Fuzzy control based energy management strategy of battery/super-capacitor hybrid energy system of electric vehicles, (in Chinese), *Automot. Eng.*, vol. 41, no. 6, pp. 615–624&640, 2019.

[4] Z. Y. Song, The optimization and control of libattery/supercapacitor hybrid energy storage system for bus, PhD dissertation, Tsinghua University, Beijing, China, 2016.

[5] D. Xu, H. Zhou, B. Wang, B. G. Cao, and J. L. Wang, A simplified cascading hybrid power and its control scheme for electric vehicles, (in Chinese), *Automot. Eng.*, vol. 39, no. 12, pp. 1368–1374, 2017.

[6] Y. T. Luo, X. T. Liu, W. Q. Liu, and X. S. Ruan, Design of hybrid power system for prolonging lifespan of lithium-ion battery applied to electric vehicles, (in Chinese), *J. South China Univ. Technol.* (*Nat. Sci. Ed.*), vol. 44, no. 3, pp. 51–59, 2016.

[7] M. Ding, G. D. Lin, Z. N. Chen, Y. Q. Luo, and B. Zhao, A control strategy for hybrid energy storage systems, (in Chinese), *Proc. CSEE*, vol. 32, no. 7, pp. 1–6, 2012.

[8] J. J. Hu, Y. Zheng, Z. H. Hu, and J. Xiao, Parameter matching and control strategies of hybrid energy storage system for pure electric vehicle, (in Chinese), *China J. Highway Transp.*, vol. 31, no. 3, pp. 142–150, 2018.

[9] J. Li, Y. Z. Zhu, L. Ji, and Y. J. Xu, Optimization of fuzzy control strategy for hybrid electric vehicle, (in Chinese), *Automot. Eng.*, vol. 38, no. 1, pp. 10–14&21, 2016.

[10] G. Tan, W. Shu, Y. Guo, and M. Liu, The application of fuzzy control in brushless DC motor for pure electric vehicle, in *Proc. IEEE Int. Conf. Communication Problem-Solving* (*ICCP*), Guilin, China, 2015, pp. 560–562.

[11] Y. Li, X. Lu, and N. C. Kar, Rule-based control strategy with novel parameters optimization using NSGA-II for power-split PHEV operation cost minimization, *IEEE Trans. Veh. Technol.*, vol. 63, no. 7, pp. 3051–3061, 2014.

[12] Y. H. Cheng and C. M. Lai, Control strategy optimization for parallel hybrid electric vehicles using a memetic algorithm, *Energies*, vol. 10, no. 3, p. 305, 2017.

[13] X. S. Hu, N. Murgovski, L. M. Johannesson, and B. Egardt, Comparison of three electrochemical energy buffers applied to a hybrid bus powertrain with simultaneous optimal sizing and energy management, *IEEE Trans. Intell. Transport. Syst.*, vol. 15, no. 3, pp. 1193–1205, 2014.

[14] F. Zhou, C. X. Song, T. W. Liang, and F. Xiao, Parameter matching of on-board hybrid energy storage system using NSGA-II algorithm, (in Chinese), *J. Jilin Univ.* (*Eng. Technol. Ed.*), vol. 47, no. 5, pp. 1336–1343, 2017.

[15] Z. Song, H. Hofmann, J. Li, X. Han, X. Zhang, and M. Ouyang, A comparison study of different semi-active hybrid energy storage system topologies for electric

vehicles, *J. Power Sources*, vol. 274, pp. 400–411, 2015.
[16] Z. Chen, R. Xiong, and J. Cao, Particle swarm optimization-based optimal power management of plug-in hybrid electric vehicles considering uncertain driving conditions, *Energy*, vol. 96, pp. 197–208, 2016.
[17] S. B. Xie, K. K. Zhang, Q. K. Zhang, and H. R. Luo, Study on energy management strategy for parallel plug-in hybrid electric vehicles considering battery electric-thermal-depth-of-discharge, (in Chinese), *Automot. Eng.*, vol. 43, no. 6, pp. 791–798&832, 2021.
[18] P. Zhang, F. Yan, and C. Du, A comprehensive analysis of energy management strategies for hybrid electric vehicles based on bibliometrics, *Renew. Sust. Energ. Rev.*, vol. 48, pp. 88–104, 2015.
[19] L. Zhang, X. Hu, Z. Wang, F. Sun, J. Deng, and D. G. Dorrell, Multiobjective optimal sizing of hybrid energy storage system for electric vehicles, *IEEE Trans. Veh. Technol.*, vol. 67, no. 2, pp. 1027–1035, 2018.
[20] X. Wu, X. Yan, Y. Wang, B. X. Huang, and Z. C. Liu, Study on DC resistance characteristics of ternary lithium batteries, (in Chinese), *Chin. J. Power Sources*, vol. 43, no. 4, pp. 568–570&684, 2019.
[21] L. Zhang, X. Hu, Z. Wang, J. Ruan, C. Ma, Z. Song, D. G. Dorrell, and M. G. Pecht, Hybrid electrochemical energy storage systems: An overview for smart grid and electrified vehicle applications, *Renew. Sust. Energ. Rev.*, vol. 139, p. 110581, 2021.
[22] Q. Wang, Z. Wang, L. Zhang, P. Liu, and L. Zhou, A battery capacity estimation framework combining hybrid deep neural network and regional capacity calculation based on real-world operating data, *IEEE Trans. Ind. Electron.*, vol. 70, no. 8, pp. 8499–8508, 2023.
[23] D. T. Qin, Z. Y. Peng, Y. G. Liu, Z. H. Duan, and Y. Yang, Dynamic energy management strategy of HEV based on driving pattern recognition, (in Chinese), *China Mechan. Eng.*, no. 11, pp. 1550–1555, 2014.
[24] M. Sharafi, and T. Y. El Mekkawy, Multi-objective optimal design of hybrid renewable energy systems using PSO-simulation based approach, *Renew. Energ.*, vol. 68, pp. 67–79, 2014.
[25] L. H. Xi, X. Zhang, C. Geng, and Q. C. Xue, Energy management strategy optimization of extended-range electric vehicle based on dynamic programming, (in Chinese), *J. Traffic Transp. Eng.*, vol. 18, no. 3, pp. 148–156, 2018.
[26] S. B. Xie, T. Liu, H. L. Li, and Z. K. Xin, A study on predictive energy management strategy for a plug-in hybrid electric bus based on Markov Chain, (in Chinese), *Automot. Eng.*, vol. 40, no. 8, pp. 871–877&911, 2018.

Juanying Zhou received the BEng degree in vehicle engineering from Taiyuan University of Science and Technology, China in 2006, and the MEng degree in vehicle engineering from Chang'an University, China in 2009. She is currently a PhD candidate in vehicle engineering at Chang'an University, China. She has been working as an associate professor at College of Automotive Engineering and General Aviation, Shaanxi Vocational and Technical College since 2009. She had applied for six patents, among which three have been authorized. She has published over 10 papers featuring her research interests in theory and optimal energy control strategies for hybrid EVs.

Lufeng Wang received the BEng degree in management from Chang'an University, China in 2007, and the MEng degree in vehicle engineering from the same university in 2017. He has been working as a lecturer at College of Automobile, Shaanxi College of Communication Technology, China since 2017. He has applied for five patents, among which three have been authorized. He has published seven papers. His research interests include hybrid vehicles, and theory and optimal energy control strategies for hybrid EVs.

Jianyou Zhao received the PhD degree from Chang'an University, China. He is a professor and doctoral supervisor at Chang'an University. He has been an assistant professor at Mechanical Engineering Department, Texas AM University, USA. He has published more than 150 papers in authoritative Chinese journals, including *Journal of Traffic and Transportation Engineering*, *Journal of Chang'an University* (*Nature Science Edition*), *Journal of Safety Science and Technology*, *Journal of Safety and Environment*, and international journals, such as *Journal of Ambient Intelligence and Humanized Computing*, *Journal of Advanced Transportation*, and *Transportation Research Part F-Traffic Psychology and Behaviour*. He has 70 authorized inventions. Furthermore, he has authored three books, and has presided over and participated in more than 20 scientific research projects from the Natural Science Foundation, State 863 Plan Project, and Western Transportation, among others. He has won three provincial awards and six national patents. He is also a member of the China Society of Automobile, China Society of Human Engineering, Shaanxi Highway Society, and China Library Society. His research interests in theory and optimal energy control strategies for hybrid EVs.